10-13-2010

Membrane anchoring subunits specify selective regulation of RGS9·Gbeta5 GAP complex in photoreceptor neurons

Yan Cao
University of Minnesota, Minneapolis

Alexander V. Kolesnikov
Washington University School of Medicine in St. Louis

Ikuo Masuho
University of Minnesota, Minneapolis

Vladimir J. Kefalov
Washington University School of Medicine in St. Louis

Kirill A. Martemyanov
University of Minnesota, Minneapolis

Cellular/Molecular

Membrane Anchoring Subunits Specify Selective Regulation of RGS9·Gβ5 GAP Complex in Photoreceptor Neurons

Yan Cao,[1] Alexander V. Kolesnikov,[2] Ikuo Masuho,[1] Vladimir J. Kefalov,[2] and Kirill A. Martemyanov[1]

[1]Department of Pharmacology, University of Minnesota, Minneapolis, Minnesota 55455, and [2]Department of Ophthalmology and Visual Sciences, Washington University in St. Louis, St. Louis, Missouri 63110

The RGS9·Gβ5 complex is the key regulator of neuronal G-protein signaling and shows remarkable selectivity of subunit composition. In retinal photoreceptors, RGS9·Gβ5 is bound to the membrane anchor R9AP and the complex regulates visual signaling. In the basal ganglia neurons, RGS9·Gβ5 is instead associated with a homologous protein, R7BP, and regulates reward circuit. Switching this selective subunit composition of the complex in rod photoreceptors allowed us to study the molecular underpinning of signaling specificity in diverse G-protein pathways. We have found that both membrane anchoring subunits play a conserved role in regulating protein levels of RGS9·Gβ5 and enhancing the ability of RGS·Gβ5 complexes to stimulate GTPase activity of G proteins. However, notable differences exist in the subcellular targeting of alternatively configured complexes. Unlike R9AP, which relies on passive targeting mechanisms for the delivery to the outer segments of the photoreceptors, R7BP is excluded from this location and is instead specifically targeted to the plasma membrane. R7BP-containing complexes could be rerouted to the outer segments, where they are capable of regulating the phototransduction cascade by the active targeting signals derived from rhodopsin. These findings illustrate the diversity of the G-protein signaling regulation by RGS·Gβ5 complexes achieved by differential recruitment of the membrane anchors.

Introduction

The R7 family of regulators of G-protein signaling proteins (R7 RGS) plays pivotal roles in controlling several fundamental neuronal processes (such as vision, nociception, and locomotion) in mammals (Anderson et al., 2009). The four members of the family, RGS6, RGS7, RGS9, and RGS11, are enriched in neurons where they facilitate termination of the G-protein-coupled receptor responses by accelerating the GTPase activity of the α subunits of the Gi/o proteins (Hooks et al., 2003). All R7 RGSs are multidomain proteins that form obligate complexes with Gβ5, an atypical G-protein β subunit (Sondek and Siderovski, 2001). Recent studies indicate that R7 RGS·Gβ5 dimers associate with two proteins: RGS9 anchor protein (R9AP) and R7 family binding protein (R7BP) (Hu and Wensel, 2002; Drenan et al., 2005; Martemyanov et al., 2005). Interestingly, R7BP and R9AP show essentially nonoverlapping expression patterns that result in differential composition of the RGS complexes with either R7BP or R9AP (Hu and Wensel, 2002; Song et al., 2007; Grabowska et al., 2008; Cao et al., 2009).

The most vivid example of the alternative complex configuration is presented by RGS9, which is highly enriched in retinal photoreceptors and striatal neurons (Martemyanov and Arshavsky, 2009; Traynor et al., 2009). In photoreceptors, RGS9-1·Gβ5 complexes with R9AP and determines the duration of the light responses by regulating the lifetime of G-protein transducin in a phototransduction cascade that relays signals from the light-activated receptor rhodopsin (Chen et al., 2000; Krispel et al., 2006). In the striatal neurons, RGS9-2·Gβ5 is instead bound to R7BP and controls signaling via μ-opioid and D2 dopamine receptors that mediate reward processing and motor control (Rahman et al., 2003; Zachariou et al., 2003; Kovoor et al., 2005; Blundell et al., 2008). Elimination of RGS9-1 (Chen et al., 2000) or disrupting its complex formation with R9AP (Keresztes et al., 2004) profoundly prolongs the recovery of photoreceptors from light excitation and results in the loss of temporal resolution (Nishiguchi et al., 2004). Similarly, disruption of RGS9-2 or R7BP substantially enhances the sensitivity of the D2 and μ-opioid receptors to stimulation by addictive drugs (Rahman et al., 2003; Zachariou et al., 2003), causes marked motor coordination deficits (Blundell et al., 2008), and is thought to exacerbate the development of dyskinesias (Kovoor et al., 2005; Gold et al., 2007).

Both R9AP and R7BP play pivotal roles in localization of RGS9·Gβ5 complexes and protecting them from rapid proteolytic degradation in their respective cells (Jayaraman et al., 2009; Martemyanov and Arshavsky, 2009). However, the significance of differential complex composition based on recruitment of the alternative anchoring subunits R7BP or R9AP remains unknown. Furthermore, it is unknown whether R7BP and R9AP provide differential contribution to the regulation of the diverse G-protein pathways controlled by RGS9·Gβ5 complexes. In this study, we used photoreceptor cells as a well studied model to directly compare the expression, subcellular targeting, and functional regulation of

Received March 8, 2010; revised Aug. 18, 2010; accepted Aug. 18, 2010.

This work was supported by NIH Grants EY018139 (K.A.M.), DA026405 (K.A.M.), EY019312 (V.J.K.), and EY02687 (Washington University, Department of Ophthalmology); McKnight Land-Grant Professorship Award (K.A.M.); Career Development Award from Research to Prevent Blindness (V.J.K.); and Karl Kirchgessner Foundation (V.J.K.). We thank Dr. Sheila Baker (University of Iowa) for critical comments on the manuscript and Dr. William Simonds (NIH) for the generous gift of anti-Gβ5 antibodies.

Correspondence should be addressed to Dr. Kirill Martemyanov, Department of Pharmacology, 6-120 Jackson Hall, 321 Church Street SE, Minneapolis, MN 55455. E-mail: martemyanov@umn.edu.

DOI:10.1523/JNEUROSCI.1191-10.2010

 0270-6474/10/3013784-10$15.00/0

RGS9·Gβ5 complexes containing either R7BP or R9AP subunits *in vivo* in the context of the physiologically well defined phototransduction cascade of the rod photoreceptors.

Materials and Methods

Antibodies, DNA constructs and mouse strains. Generation of rabbit anti-R9AP (against amino acids 144-223) (Keresztes et al., 2003) and sheep anti-RGS9c (Makino et al., 1999) antibodies was described previously. Rabbit anti-Gβ5 and rabbit anti-R7BP antibodies were gifts from Dr. William Simonds [National Institute of Diabetes and Digestive and Kidney Diseases, National Institutes of Health (NIH), Bethesda, MD]. Mouse monoclonal anti-β-actin (clone AC-15; Sigma), rabbit anti-Gαt1 (K20; Santa Cruz Biotechnology) were purchased.

Generation and characterization of mouse knock-out strains with targeted disruption of R9AP (R9AP$^{-/-}$) (Keresztes et al., 2003) and RGS9 (RGS9$^{-/-}$) (Chen et al., 2000) was described previously. For the generation of R7BP transgenic mice, the coding region of mouse R7BP gene was placed immediately after 4.4 kb mouse rhodopsin promoter (Lem et al., 1991). Following pronuclear injections into oocytes derived from C57BL/6×SJL mice, transgenic-positive founders were crossed with R9AP$^{-/-}$ mice. R7BP/rhodopsin chimera containing N-terminal portion of R7BP (amino acids 1-241) and C-terminal sequence of mouse rhodopsin (amino acids 312-348), and R7BP/R9AP chimera containing N-terminal portion of R7BP (amino acids 1-241) and C-terminal transmembrane segment of mouse R9AP (amino acids 220-237) were generated by overlap extension PCR strategy. Transgenic-negative littermates were used as controls in all experiments. Procedures involving mice strictly followed NIH guidelines and were approved by IUCUC committees at the University of Minnesota, Minneapolis, MN and Washington University in St. Louis, St. Louis, MO.

Western blotting and immunoprecipitation. Immunoprecipitation of RGS9 from retinas was performed essentially as described previously (Song et al., 2007). Whole retinas were lysed in PBS (Invitrogen) supplemented with 150 mM NaCl, 1% Triton X-100 and complete protease inhibitor tablets (Roche) by sonication on ice. Cleared lysates were incubated with sheep anti-RGS9-1 antibodies and 20 μl of 50% protein G beads (GE Healthcare) for 1 h at 4°C. Total protein concentration in samples was measured by BCA assay (Pierce). After three washes with ice-cold binding buffer, proteins bound to the beads were eluted with SDS-sample buffer (62 mM Tris, 10% glycerol, 2% SDS, 5% β-ME) and analyzed by 4–20% PAGE (Lonza). Protein bands were transferred onto polyvinylidene difluoride membrane and subjected to Western blot analysis using HRP-conjugated secondary antibodies and ECL West Pico (Pierce) detection system. For the quantitative analysis, Western blotting was performed with IRDye 680- and IRDye 800-labeled secondary antibodies and the signal was detected by Odyssey infrared imaging system (LI-COR Biosciences).

Immunohistochemistry. Dissected eyecups were fixed for 15 min in paraformaldehyde (4% in PBS), cryoprotected with 30% sucrose in PBS for 2 h at room temperature, and embedded in OCT. Frozen sections (12 μm) were obtained and blocked in PT1 (1×PBS with 0.1% Triton and 10% goat serum) for 1 h and incubated with primary antibody in PT2 (1×PBS with 0.1% Triton and 2% goat serum) for 1 h, washed four times with PT2, and incubated with Alexa 488-conjugated secondary antibodies in PT2 for 1 h. For R9AP/R7BP double staining, R7BP primary antibodies were directly labeled with Dylight 549 using Microscale antibody labeling kit (Thermo Scientific) as previously described (Cao et al., 2008). Images were taken by the Olympus Fluoview 1000 confocal microscope.

Single-cell electrophysiology. Mouse rod outer segment membrane currents were recorded as described previously (Shi et al., 2007). Briefly, 2–3 months old animals were dark-adapted overnight, killed by CO_2 asphyxiation, and retinas were removed under infrared illumination. A single rod outer segment was drawn into a glass microelectrode filled with solution containing the following (in mM): 140 NaCl, 3.6 KCl, 2.4 $MgCl_2$, 1.2 $CaCl_2$, 3 HEPES, pH 7.4, 0.02 EDTA, and 10 glucose. Cells were perfused with solution containing the following (in mM): 112.5 NaCl, 3.6 KCl, 2.4 $MgCl_2$, 1.2 $CaCl_2$, 10 HEPES, pH 7.4, 20 $NaHCO_3$, 3 Na succinate, 0.5 Na glutamate, 0.02 EDTA, and 10 glucose. The perfusion solution was continuously bubbled with 95% O_2/5% CO_2 mixture and heated to 37–38°C.

Light stimulation was applied by 20 ms test flashes of calibrated 500 nm light. Photoresponses were amplified, low-pass filtered at 30 Hz (8-pole Bessel), digitized at 1 kHz, and stored on a computer for further analysis. Half-saturating light intensity ($I_{1/2}$) was calculated from the intensity-response relation for each cell as the test flash intensity required to produce a response with an amplitude equal to half of the corresponding saturated response. Integration time was calculated as the time integral of the dim flash response with the transient peak amplitude normalized to unity. Time constant of the dim flash response recovery (τ_{rec}) was derived from single-exponential fit to the falling phase of the response. Dominant recovery time constant (τ_D) was determined from supersaturating flashes as described previously (Pepperberg et al., 1992). The time in saturation was defined as the time between the midpoint of the flash and the point at which photocurrent recovered by 20%. Data were analyzed using ClampFit 10.2 and Origin 7.5 software. Data were analyzed using independent two-tailed Student's t test, with accepted significance level of $p < 0.05$, and expressed as mean ± SEM.

Protein and membrane preparations. Purification of RGS7·Gβ5S and RGS9-1·Gβ5L following the expression in Sf9/baculovirus system was described previously (Skiba et al., 2001; Martemyanov et al., 2005). Protein purity was at least 50% as judged by Coomasie staining of the gels. The $G\alpha_o\beta_1\gamma_2$ heterotrimer was expressed and purified as described previously (Masuho et al., 2010). Isolation of bovine V8-urea-treated rod outer segment membranes (Lishko et al., 2002) and insect cell membranes (Masuho et al., 2010) was also described. Sf9 membranes containing recombinant R7BP were purified following baculovirus-mediated expression of R7BP chimera supplemented with R9AP transmembrane segment [R7BP(R9APCT)].

Mouse ROS disc membranes were prepared following procedure described by Tsang et al. (1998). The retinas were snap frozen with liquid nitrogen and stored at −80°C until use. Mouse ROS were isolated in Ringer's solution containing the following (in mM):130 NaCl, 3.6 KCl, 2.4 $MgCl_2$, 1.2 $CaCl_2$, 10 HEPES with NaOH, pH 7.4, 0.02 EDTA, and complete protease inhibitor mixture (Roche), and ionic strength was adjusted to 313 mOsm. Before conducting GTPase assays, ROS were resuspended in 45 μl of water following adjustment of osmolarity by adding 5 μl of a 10× GTPase buffer containing 1 M NaCl, 80 mM $MgCl_2$, 100 mM Tris with HCl, pH 7.8. The ROS were snap frozen with liquid nitrogen and stored at −80°C. All procedures were performed under dim red light illumination.

GTPase assays. Single-turnover GTPase assays using mouse ROS were performed as described previously (Tsang et al., 1998), with minor modifications. Briefly, GTPase reaction was started by mixing bleached ROS (14 μl) containing 37.5 μM rhodopsin with 7 μl of 0.6 μM [γ-^{32}P]GTP, and the time course of ^{32}Pi (Pi, inorganic phosphate) formation was determined by the activated charcoal assay after the samples were quenched with perchloric acid.

Single-turnover GTPase assays using bovine uROS and recombinant proteins were conducted as described previously (Martemyanov and Arshavsky, 2004). Assays were performed at room temperature in GTPase buffer (10 mM Tris-HCl pH 7.4, 250 mM NaCl, 8 mM MgCl, and 1 mM DTT). Final concentrations in the reactions were 20 μM rhodopsin, 1.0 μM $G\alpha_o\beta_1\gamma_2$ heterotrimer, 50 nM RGS7·Gβ5, and 5 mg/ml Sf9 or R7BP membrane preparations. The reaction was stopped by the addition of 100 μl of 6% perchloric acid. Phosphate released from hydrolyzed GTP was determined by activated charcoal assay (Cowan et al., 2000). Control experiments were performed to ensure that single turnover conditions are maintained and that GDP/GTP exchange is not limiting the GTP hydrolysis (Cowan et al., 2000; Martemyanov and Arshavsky, 2004).

Results

Transgenic expression of R7BP in rod photoreceptors provides an alternative subunit for the association with RGS9-1·Gβ5 complex

Previous studies have established that R7BP is not present in the photoreceptors and thus RGS9-1·Gβ5 complex in these neurons

is associated solely with R9AP (Song et al., 2007). To study the behavior of RGS9-1·Gβ5 when both membrane targeting subunits are available for binding in the same cell, we have transgenically expressed R7BP in rod photoreceptors of the mouse. The expression was driven by the 4.4 kb mouse rhodopsin promoter (Fig. 1*A*) that resulted in selective targeting of rods, as demonstrated by immunohistochemical analysis (Fig. 1*B*). Transgenic expression did not affect overall retinal morphology and no signs of degenerative changes were evident (Fig. 1*A*). Two independent lines with varying degrees of R7BP expression were generated. In both lines, the levels of R7BP in photoreceptors were substantially above the levels of endogenous protein, which is normally found in the inner retina. Analysis of protein expression by quantitative Western blotting revealed that R7BP content in low- [TgR7BP(L)] and high- [TgR7BP(H)] expressing lines was increased ~3- and 13-fold above the endogenous levels in the inner retina, respectively (Fig. 1*C*,*D*). Importantly, transgenic expression of R7BP resulted in the concomitant elevation in the levels of both RGS9-1 and long-splice isoform of Gβ5. This observation leads to the conclusion that levels of transgenic R7BP are comparable to the levels of endogenous R9AP and that R7BP provides further proteolytic protection to the RGS9-1·Gβ5 complex.

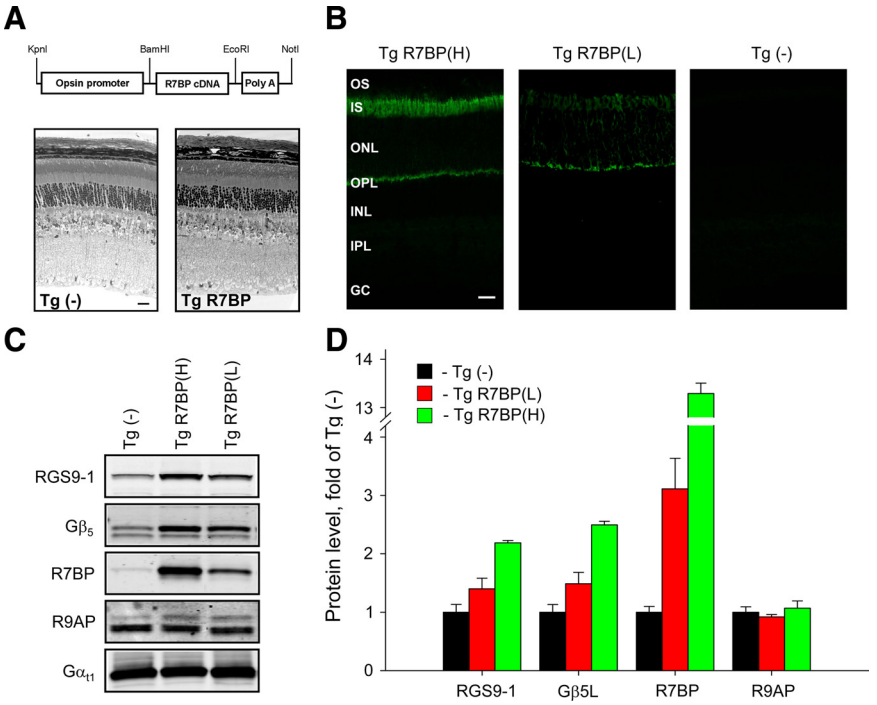

Figure 1. Transgenic expression of R7BP in rod photoreceptors. ***A***, Top, Schematics of the genetic construct used to target R7BP expression to rod photoreceptors. Bottom, Ultrathin sections of plastic-embedded retinas from 2-month-old transgenic (Tg R7BP) and nontransgenic littermates [Tg(−)] showing normal retina morphology. Scale bar is 25 μm. ***B***, Immunohistochemical detection of R7BP expression in cross-sections of retinas from transgenic mice that express either high [R7BP(H)] or low [R7BP(L)] levels of R7BP compared with nontransgenic littermates. OS, Outer segment; IS, inner segment; ONL, outer nuclear layer; OPL, outer plexiform layer; INL, inner nuclear layer; IPL, inner plexiform layer; GC, ganglion cell layer. Scale bar is 20 μm. ***C***, Analysis of protein expression in the retinas of transgenic mice by Western blotting. Into each lane was loaded 8.5 μg of total protein and the blots were probed with the indicated antibodies. ***D***, Quantification of the Western blot data presented in ***C***. Protein band intensities were determined by Odyssey infrared imaging system software package. Values from three independent experiments were averaged and plotted after normalization to the levels found in nontransgenic animals. Error bars represent SEM values.

Direct analysis of the complex formation by immunoprecipitation assays revealed that RGS9-1·Gβ5 readily forms complexes with transgenic R7BP (Fig. 2*A*). Furthermore, increase in the concentration of R7BP in the rods caused progressive decline in the ability of RGS9-1 to coprecipitate with R9AP, indicating that, in transgenic rods, two membrane anchors compete for the RGS9-1·Gβ5 binding. Indeed, quantitative analysis of the complex composition revealed that, despite unaltered concentration of R9AP, most of the RGS9-1·Gβ5 exists in complex with R7BP (Fig. 2*B*).

R9AP and R7BP demonstrate nonoverlapping, subcellular localization patterns

Examination of transgenic R7BP localization in photoreceptors by immunostaining demonstrated that it is found throughout the cell body and is present in axonal terminals but appears to be completely excluded from the outer segments, a ciliary compartment harboring the components of the phototransduction cascade (Fig. 3*A*). In contrast, as previously documented (Hu and Wensel, 2002; Martemyanov et al., 2003), R9AP is exclusively seen in photoreceptor outer segments. Analysis of R7BP and R9AP distribution by dual immunolabeling confirmed a nonoverlapping localization of the two membrane anchors in rods (Fig. 3*A*). Examination of R7BP localization at higher magnification detected its association with the plasma membranes of the cells, which was particularly evident in the inner segments (Fig. 3*B*). Interestingly, we found no evidence for the presence of R7BP in the nucleus (Fig. 3*A*,*B*), a presumed alternative localization site of R7BP (Drenan et al., 2005; Song et al., 2006; Panicker et al., 2010). Together, these findings indicate that, despite their homologous nature and conserved complex formation with RGS9-1·Gβ5, R7BP and R9AP exhibit very different localization patterns in a model neuronal cell—the rod photoreceptor.

Transgenic replacement of R7BP for R9AP rescues RGS9-1·Gβ5 expression but mistargets the complex

The expression of RGS9- ·Gβ5 has been shown to be dependent on R9AP as no detectable RGS9-1 is found in the absence of R9AP (Keresztes et al., 2004). Elevation of the RGS9-1·Gβ5 levels in R7BP transgenic animals (Fig. 1*C*,*D*) suggests that R7BP can replace R9AP in providing proteolytic protection to the complex. To test this possibility, we out-bred the transgenic lines into the R9AP$^{-/-}$ background. As previously reported, we found no RGS9-1 present in the retinas of R9AP$^{-/-}$ mice (Fig. 4*A*). However, transgenic introduction of R7BP into rods of R9AP$^{-/-}$ resulted in the complete restoration of RGS9-1 expression in retinas of the high expressor line and ~50% recovery in the transgenic line expressing lower amounts of R7BP (Fig. 4*B*). This result indicates that R7BP can effectively substitute for R9AP in protecting RGS9-1·Gβ5 complex from proteolytic degradation. We next analyzed the effect of the transgenic substitution on the localization of RGS9-1 in the photoreceptors. Consistent with the differential targeting of R7BP and R9AP and their competition for RGS9-1 binding, we found that expression of R7BP delocalizes a substantial fraction of RGS9-1 away from the outer segments (Fig. 4*C*). Furthermore, in the retinas of R9AP$^{-/-}$ mice

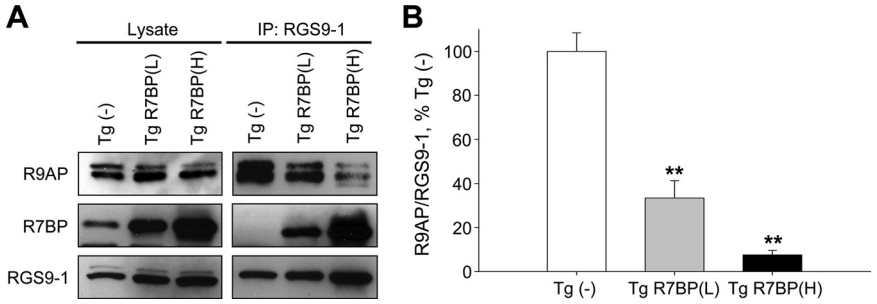

Figure 2. R9AP and R7BP compete for binding to RGS9-1 in transgenic retinas. ***A***, Analysis of protein levels in transgenic retinas before and after RGS9-1 immunoprecipitation. Lower amounts of R9AP coprecipitate with RGS9-1 in transgenic retinas containing higher levels of R7BP. All retinas are from mice of R9AP $^{+/-}$ background. ***B***, Quantification of data presented in ***A***. The ratios between R9AP and RGS9-1 band intensities in the eluate fractions after immunoprecipitation are plotted. Error bars represent SEM values. $^{**}p < 0.01$, *t* test; statistically significant difference in ratios compared with nontransgenic littermates.

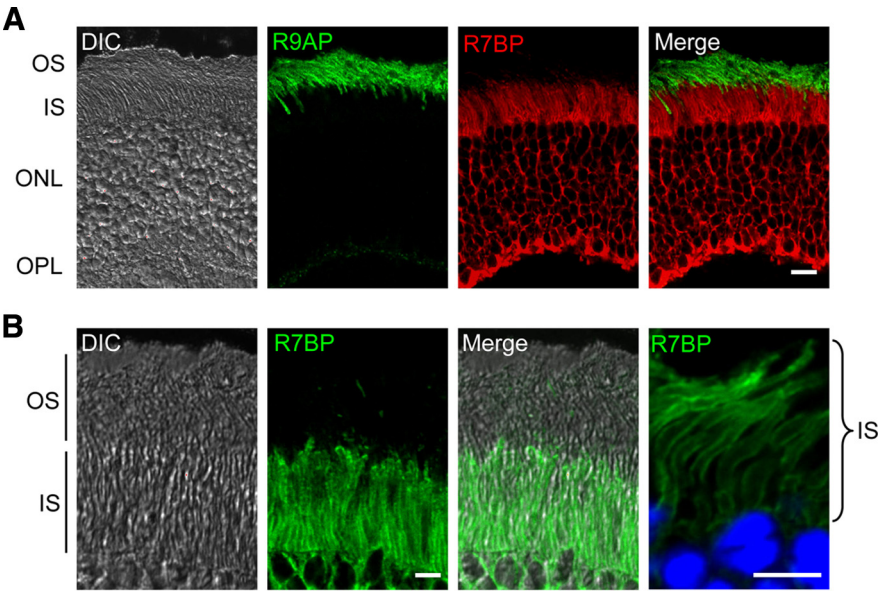

Figure 3. Differential targeting of R7BP and R9AP in rods. ***A***, Immunohistochemical analysis of R7BP and R9AP localization in photoreceptors of R7BP(H) transgenic mice. Retinas were double stained with R7BP (red) and R9AP (green) antibodies, as described in Materials and Methods, and fluorescence was determined by confocal microscopy. Scale bar is 10 μm. ***B***, Higher magnification of photoreceptor outer and inner segment region showing exclusive plasma membrane localization of R7BP in the inner segment. Nuclei are labeled by DAPI and appear in blue channel. Scale bar is 5 μm. OS, Outer segment; IS, inner segment; ONL, outer nuclear layer; OPL, outer plexiform layer; DIC, differential interference contrast.

when only R7BP is present in the photoreceptors, no RGS9-1 can be found in the outer segments, indicating targeting of RGS9-1 complex in the cell is entirely dependent on its association with its membrane anchors (Fig. 4*C*).

The C-terminal sequence from rhodopsin, but not from R9AP, provides R7BP with an outer segment targeting signal

Our results indicate that, despite structural similarity to R9AP, which is resident to the outer segments, R7BP is excluded from this location. To gain insight into the mechanisms of selective protein targeting in the photoreceptors, we have performed site-directed mutagenesis aimed at altering the subcellular destination of R7BP. The C terminus of R7BP was replaced by the C-terminal transmembrane domain of R9AP, which can passively promote outer segment localization (Baker et al., 2008), or C-terminal sequence of rhodopsin, which contains an active outer segment targeting signal (Tam et al., 2000; Deretic et al., 2005). The resulting constructs (Fig. 5*A*) were used to generate transgenic mice. Examination of the chimeric R7BP mutant's localization patterns in transgenic retinas revealed that the transmembrane segment from R9AP did not significantly change the targeting of R7BP [TgR7BP(R9APCT)], which was still essentially excluded from the outer segments (Fig. 5*B*). In contrast, when supplemented with the C terminus of rhodopsin, a significant fraction of R7BP [TgR7BP(RhoCT)] was found to be present in the outer segments, where it was colocalized with R9AP (Fig. 5*B*; supplemental Fig. 1, available at www.jneurosci.org as supplemental material). Notably, we have observed that R7BP(RhoCT) protein was distributed in a gradient fashion with most of the protein being concentrated within basal ~1/3 of the outer segment and its concentration gradually declining toward the distal end of the cell (supplemental Fig. 1 and supplemental movie, available at www.jneurosci.org as supplemental material). Within this basal portion, R7BP (RhoCT) protein was found to reside primarily in the center of the outer segment rather than at the periphery, indicative of its location on the photoreceptor disc membranes as opposed to the plasma membrane (supplemental Fig. 1, available at www.jneurosci.org as supplemental material).

We next out-bred the transgenic animals onto the R9AP $^{-/-}$ background to study the effects on expression and targeting of the RGS9-1 complex. Both mutant R7BP transgenes were able to provide proteolytic protection to RGS9-1·Gβ5 complex, as evident by the restoration of RGS9-1 expression (Fig. 5*C*). Consistent with the localization of mutant R7BP, we found that no RGS9-1 was delivered to the outer segments in transgenic mice expressing R7BP(R9APCT) construct (Fig. 5*D*). At the same time, substantial fraction of RGS9-1 could be found in the outer segments of the R7BP(RhoCT) rods (Fig. 5*D*).

To quantitatively assess the targeting of the RGS9-1 complex in transgenic photoreceptors, we purified rod outer segments and compared RGS9-1 content between preparations obtained from wild-type and R7BP(RhoCT) transgenic retinas. A standard curve with recombinant RGS9-1·Gβ5 complex spiked into rod outer segment preparations derived from RGS9 $^{-/-}$ retinas was used to correct for the nonlinearity of RGS9-1 detection by Western blotting (Martemyanov et al., 2008). Analysis of the data presented in Figure 5*E* indicates that outer segments of R7BP(RhoCT) rods contain approximately eight times less RGS9-1 compared with wild-type rod outer segments (1.6 ± 0.2 fmol vs 12.7 ± 2.8 fmol per 1 pmol of rhodopsin, respectively; $n = 2$, errors represent a range of the experimental variability). We therefore conclude that, al-

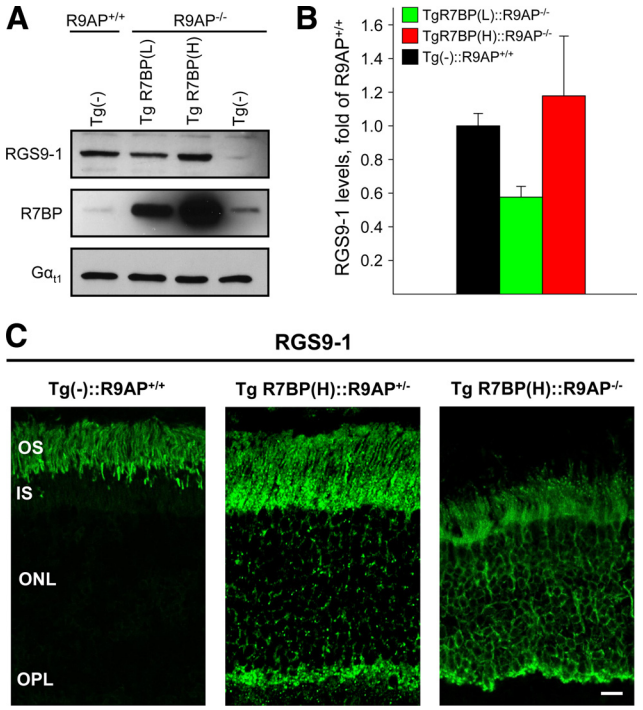

Figure 4. Critical role of R7BP and R9AP in targeting RGS9-1·Gβ5 to alternative locations in photoreceptors. ***A***, Western blotting analysis of the protein expression in transgenic retinas of R9AP $^{-/-}$ background. Transducin ($G\alpha_{t1}$) detection was used as the loading control. ***B***, Quantification of data presented in ***A*** showing that expression of transgenic R7BP can rescue proteolytic instability of RGS9-1 in R9AP $^{-/-}$ retinas. RGS9-1 band intensities were normalized to $G\alpha_{t1}$ content and reflected as fold change over RGS9-1 present in transgenic-negative R9AP $^{+/+}$ (wild-type) samples. ***C***, Expression of R7BP in R7BP transgenic retina delocalized RGS9-1 from the outer segments of photoreceptors. Retina cross-sections were immunostained with anti-RGS9-1 antibodies as described in Materials and Methods. Scale bar is 10 μm. OS, Outer segment; IS, inner segment; ONL, outer nuclear layer; OPL, outer plexiform layer.

though rhodopsin C-terminal sequence can clearly target R7BP–RGS9-1·Gβ5 complex to the outer segments, it does not completely override the plasma membrane targeting signals intrinsic to R7BP.

Regulation of phototransduction by the RGS9-1·Gβ5·R7BP complex

Successful targeting of a portion of R7BP to the outer segments of rods permitted us to address the consequences of R7BP expression on the regulation of the phototransduction cascade. We used single-cell suction electrode recordings to compare the responses of R7BP-RhoCT (R9AP $^{-/-}$) transgenic rods to those of the transgenic-negative R9AP $^{-/-}$ littermates. Examination of response parameters (Table 1) reveals no significant difference between genotypes in the rising phases of the responses as well as the light sensitivity, defined as the half-saturating light intensity ($I_{1/2}$). Several studies documented that elimination of either of the components of RGS9-1·Gβ5·R9AP complex in mouse rods severely delays the falling phase of the photoresponse, reflecting slower phototransduction inactivation in the absence of the GAP activity (Chen et al., 2000; Krispel et al., 2003; Keresztes et al., 2004; Pugh, 2006). Indeed, we observed very slow deactivation kinetics in transgenic-negative (R9AP $^{-/-}$) photoreceptors (Fig. 6*A*), in complete agreement with previously published observations. Since the deactivation phase of the response is very sensitive to changes in the expression level of the RGS9-1 complex (Burns and Pugh, 2009), we next performed a detailed analysis of both dim flash and saturating response kinetics in R7BP(RhoCT) transgenic rods. We found that R7BP(RhoCT) rods showed a modest (~15%) but statistically significant ($p < 0.01$, *t* test) acceleration in the dim flash recovery time constant (τ_{rec}) compared with their nontransgenic R9AP $^{-/-}$ littermates (Table 1, Fig. 6*C*). Furthermore, the dominant time constant of photoresponse recovery after a series of supersaturating flashes (τ_D) (Fig. 6*D*, Table 1) was also accelerated by ~23% ($p < 0.01$, *t* test). Considering that R7BP transgenic photoreceptors contain only 12% of RGS9-1 content normally found in wild-type rod outer segments, these data indicate that RGS9-1·Gβ5 complexed with R7BP is capable of accelerating the phototransduction inactivation.

Stimulation of the GAP activity of R7 RGS proteins on Gα is a general mechanism of R7BP action

Speeding up the kinetics of photoresponse shutoff in R7BP(RhoCT) rods suggests that R7BP acts to promote the GAP activity of RGS9-1·Gβ5 complex on transducin. To directly test this possibility, we performed single-turnover GTPase assay with rod outer segments purified from wild-type, R9AP $^{-/-}$, and R7BP(RhoCT) transgenic retinas. We found that the rate of transducin GTPase activity was substantially slower in R9AP $^{-/-}$ preparations (Fig. 7*A*,*B*). This decrease in the GTPase activity is of similar magnitude to that found in RGS9 $^{-/-}$ outer segment preparations (Chen et al., 2000) and is consistent with the lack of detectable RGS9-1 expression. At the same time, transducin GTPase rates were significantly higher in R7BP(RhoCT) compared with R9AP $^{-/-}$ preparations. Subtracting the rate of unstimulated GTPase activity observed in R9AP $^{-/-}$ preparations allowed us to calculate the GAP activity mediated by R9AP-containing complexes (wild-type preparations) to be $3.8 \pm 0.8 \times 10^{-2}$ s $^{-1}$ and the activity mediated by R7BP-containing complexes [R7BP(RhoCT) preparations] to be $9.9 \pm 2.5 \times 10^{-3}$ s $^{-1}$. The lower GAP activity observed in R7BP-transgenic outer segments parallels lower expression level of RGS9-1 and slower termination kinetics in these rods. We therefore conclude that speeding up of the photoresponse deactivation upon expression of R7BP is directly attributed to the ability of the RGS9-1·Gβ5·R7BP complex to facilitate the GTPase activity of transducin.

R7BP is naturally expressed throughout the nervous system (Martemyanov et al., 2005; Grabowska et al., 2008) where, in addition to RGS9-1, it forms complexes with other R7 RGS proteins (Drenan et al., 2005; Martemyanov et al., 2005) that regulate the activity of G-proteins other than transducin. Thus, we investigated whether stimulation of the GAP activity of RGS proteins could be a general action of R7BP. This question was addressed by studying the effects of R7BP on the GAP activity of RGS7·Gβ5, a ubiquitously expressed homolog of RGS9, toward $G\alpha_o$. In an *in vitro* reconstituted system, the ability of RGS7·Gβ5 to stimulate $G\alpha_o$ GTP hydrolysis was found to be threefold higher in the membrane preparations reconstituted with R7BP (Fig. 7*C*,*D*). These observations suggest that R7BP is a general regulator of R7 RGS GAP activity in addition to its roles in mediating protein targeting and proteolytic stabilization.

Discussion

In the current study, we have examined the impact of altering the membrane-anchoring subunits R7BP and R9AP on the expression, subcellular localization, and activity regulation of a key G-protein signaling regulator, RGS9-1, in the *in vivo* model of mammalian rod photoreceptors. The results of the study allow us to draw several important conclusions about the mechanisms of

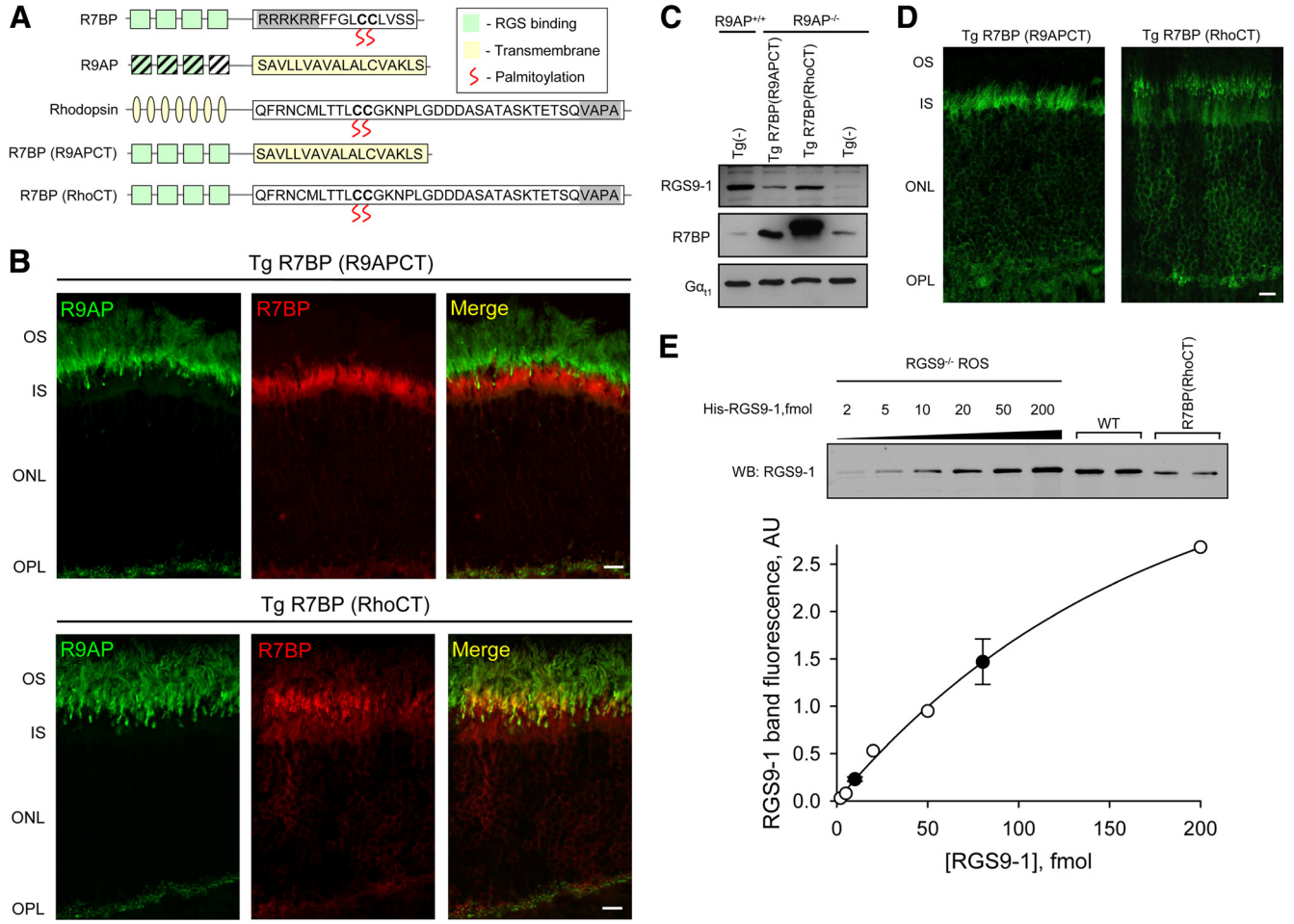

Figure 5. Reconstitution of the RGS9-1·Gβ5·R7BP complex in the outer segments of the rod photoreceptors. ***A***, Schematic illustration of targeting signals replaced in R7BP. The C terminus of R7BP was replaced by either the C-terminal signal sequence from rhodopsin [R7BP(RhoCT)] or from R9AP [R7BP(R9APCT)]. Constructs were used to generate transgenic mice. ***B***, Localization of chimeric R7BP proteins in transgenic photoreceptors. Retinas were double stained for R7BP and R9AP. R9AP staining was used as a marker for the outer segments. Colocalization of proteins is revealed by yellow fluorescence when overlaying the green (R9AP) and red (R7BP) detection channels. Images were obtained by confocal microscopy. Scale bar is 10 μm. ***C***, Expression of chimeric R7BP constructs rescues RGS9-1 levels in R9AP $^{-/-}$ retinas. Protein expression was analyzed by Western blotting with indicated antibodies. ***D***, RGS9-1 is delivered to the outer segments of R7BP(RhoCT) transgenic mice but remains primarily in the inner segments of R7BP(R9APCT) photoreceptors. Retina cross-sections were stained with the antibodies against RGS9-1 and fluorescence was detected by confocal microscopy. Scale bar is 10 μm. ***E***, Quantification of RGS9-1 content in the outer segments isolated from transgenic retinas by Western blotting. Varying amounts of purified recombinant RGS9-1·Gβ5 protein were spiked into outer segments isolated from RGS9 $^{-/-}$ retinas (5 pmol of rhodopsin/lane) and RGS9-1 band intensities were determined by Western blotting in parallel with the outer segment samples obtained from transgenic and wild-type mice. Values obtained from recombinant RGS9-1 band intensities (open circles) were used to generate a standard curve. RGS9-1 band intensities from the samples in question: wild type (WT) and R7BP(RhoCT) were plotted on the calibration curve (closed circles) and used to determine RGS9-1 concentration. The experiment was performed two times. Error bars represent the scatter of the data. OS, Outer segment; IS, inner segment; ONL, outer nuclear layer; OPL, outer plexiform layer.

Table 1. Electrophysiological parameters of the rod photoreceptor responses to light

Genotype	I_{dark} (pA)	$I_{1/2}$ (ph μm^{-2})	T_{peak} (ms)	T_{integr} (s)	τ_{rec} (s)	τ_D (s)
Tg(−) R9AP $^{-/-}$	9.1 ± 0.4 (26)	100 ± 18 (5)	134 ± 4 (26)	2.2 ± 0.1 (26)	2.7 ± 0.2 (26)	9.7 ± 0.5 (26)
R7BP(RhoCT) R9AP $^{-/-}$	11.3 ± 0.5 (31)	123 ± 12 (21)	154 ± 3 (22)	2.1 ± 0.1 (22)	2.3 ± 0.2 (22)	7.5 ± 0.4 (31)

G-protein signaling regulation and subcellular protein targeting in polarized cells.

Membrane anchors and catalytic activity of R7 RGS proteins

Earlier studies with the retina-specific membrane anchor R9AP indicated that it is involved in modulating the ability of the RGS9-1·Gβ5 complex to stimulate transducin GTPase (Lishko et al., 2002; Hu et al., 2003). A more recent study provided evidence that R9AP can additionally potentiate the activity of a related RGS protein, RGS11 on $G\alpha_o$ (Masuho et al., 2010). Given the widespread expression of R7 family members, and the fact that expression of R9AP is restricted to the retina, the critical question has been how the activity of R7 RGS proteins is regulated when R9AP is unavailable. Early clues were provided by the identification of the ubiquitously expressed R7BP, an R9AP homolog that forms complexes with all four R7 RGS proteins (Drenan et al., 2005; Martemyanov et al., 2005) and by demonstrating that R7BP can potentiate RGS7 action in terminating signaling from m2 receptors to GIRK channels (Drenan et al., 2006). However, until this study, the mechanism of R7BP action on R7 RGS proteins had remained unresolved. Using direct biochemical measurements, we show that R7BP can potentiate the GAP activity of two R7 RGS proteins, RGS9-1·Gβ5 and RGS7·Gβ5, on their two G-protein substrates, $G\alpha_t$ and $G\alpha_o$, respectively. This parallels

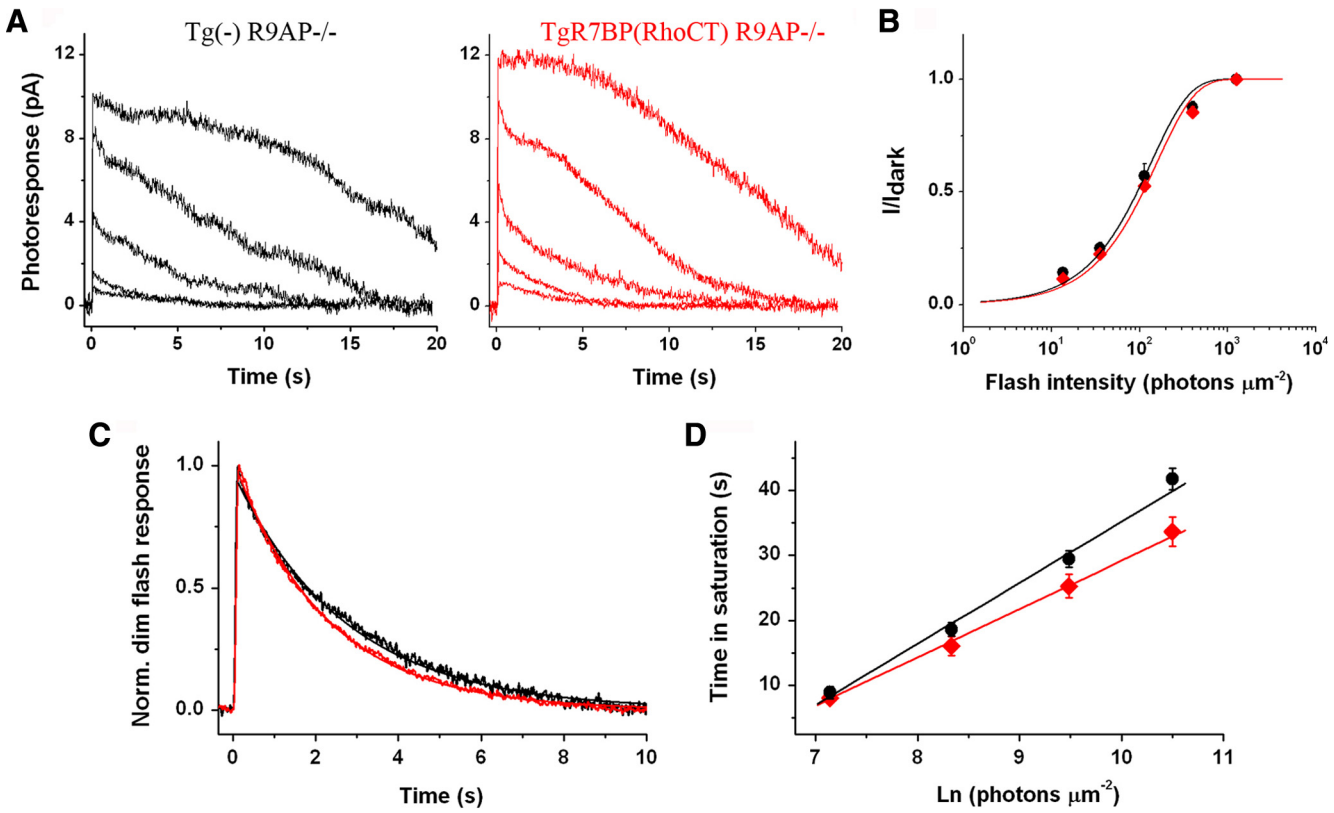

Figure 6. RGS9-1·Gβ5·R7BP complex accelerates the shutoff of the light responses. ***A***, Families of flash responses from representative transgenic-negative R9AP $^{-/-}$ (black) and R7BP(RhoCT) transgenic (red) rods. Light test flashes (500 nm) were delivered at time 0, with intensities of 14, 35, 112, 399, and 1265 photons μm^{-2}. For the representative cells shown, dark currents were 10.1 and 11.9 pA. ***B***, Normalized averaged intensity-response relations. Points were fitted with saturating exponential functions. Data are means ± SEM. ***C***, Determination of the dim flash recovery time constant. The responses were normalized to their maximum amplitudes and population-averaged (noisy lines). Light intensity for all cells was 35 photons μm^{-2}. Thin solid lines are single-exponential fits to the falling phase of responses. ***D***, Determination of the dominant time constant of recovery from a series of supersaturating flashes. Straight lines are linear fits. For parameters of fits in ***B***–***D*** see Table 1. Data are means ± SEM.

previous studies with R9AP, which was shown to stimulate the activity of RGS9-1·Gβ5 on $G\alpha_t$ (Hu et al., 2003; Martemyanov et al., 2003; Baker et al., 2006) and RGS11·Gβ5 on $G\alpha_o$ (Masuho et al., 2010). Thus, our findings indicate that stimulation of the GAP activity of the R7 RGS proteins is perhaps a universal mechanism of membrane-anchor action.

The genetic substitution of R7BP for R9AP in mammalian rod photoreceptors allowed us to use the power of well established physiological approaches to measure the contribution of R7BP to the RGS activity regulation in the native environment. In rod photoreceptors, RGS9-1·Gβ5 protein complex is a rate-limiting enzyme in the cascade of the termination reactions, leading to the recovery of the photoresponse from light excitation (Krispel et al., 2006). As such, even subtle changes in activity and/or concentration of RGS9-1·Gβ5 GAP complex are reflected in the shutoff kinetics (Burns and Arshavsky, 2005; Pugh, 2006). Indeed, evaluation of mouse models with varying RGS9-1 concentration resulted in a quantitative model describing the relationship between RGS9-1 concentration and recovery constants τ_D and τ_{rec} (Burns and Pugh, 2009). Using this model, we estimate that the 0.125× expression of RGS9-1·Gβ5 in the rods of transgenic animals would be expected to result in a τ_D value of ~2 s or ~80% speeding up of the photoresponse inactivation compared with rods lacking RGS9-1 complex. However, we found that R7BP expression results in only ~20% acceleration. This apparent lower activity of the R7BP-containing complexes might originate from their gradient distribution, which creates a situation where distal portions of the outer segments containing much lower amounts of the GAP complexes could dominate the recovery rates. Therefore, although our data clearly demonstrates that R7BP can functionally replace R9AP in contributing to the ability of the GAP complex to inactivate transducin signaling in photoreceptors, they fall short of quantitative comparisons of the catalytic activities of differentially composed complexes.

Mechanisms of RGS complex targeting in rod photoreceptors

Photoreceptor neurons represent a great model to study differential protein targeting in neurons where many signaling molecules are selectively delivered to various compartments (Deretic, 2006; Artemyev, 2008; Baker et al., 2008; Karan et al., 2008; Kizhatil et al., 2009). Our findings provide another vivid example of proteins with mutually exclusive localization pattern in the cells. Surprisingly, despite the homology with R9AP, which is targeted to the outer segments, R7BP is strictly excluded from this compartment. Recent studies proposed that proteins containing transmembrane segments are indiscriminately targeted to the outer segments via a default pathway if they lack specific signals targeting them to other cellular destinations (Baker et al., 2008). Since R7BP does not have a transmembrane segment, its failure to reach the outer segment was perhaps not surprising. However, the inability of the transmembrane domain derived from R9AP to alter the localization of R7BP indicates that it contains an active plasma membrane targeting signal. Such signal(s) can act in addition to membrane anchoring elements provided by the palmitoylated C-terminal cysteine residues to actively promote localization of the protein away from the disc membranes of the

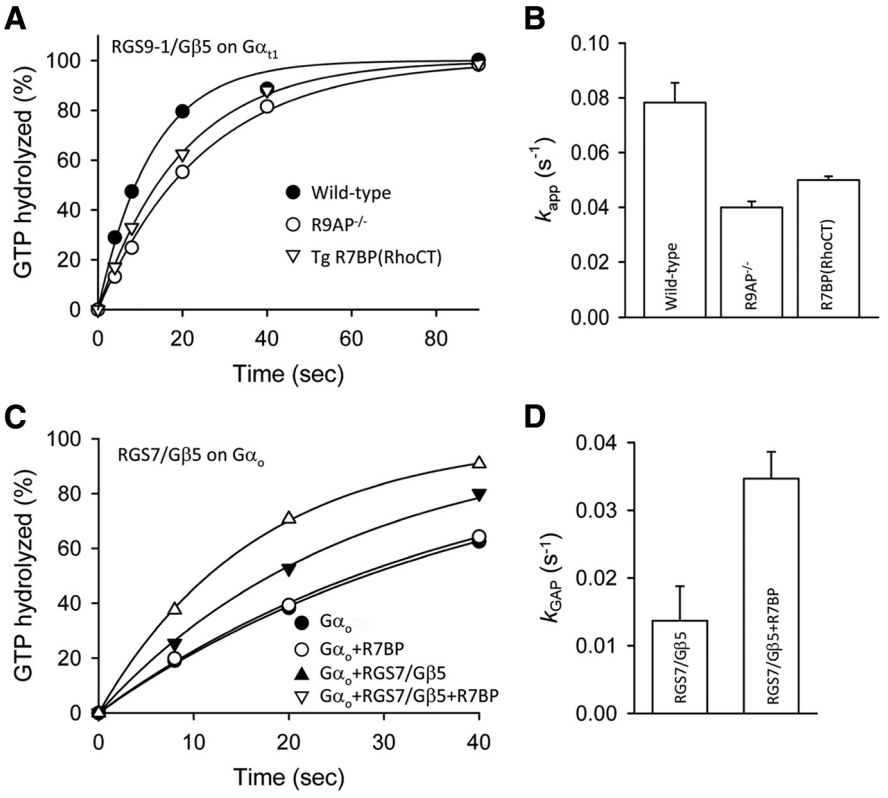

Figure 7. R7BP acts to stimulate the GAP activity of R7 RGS proteins. ***A***, GTPase activities in transgenic rod outer segments. Single-turnover GTPase activities of transducin in ROS preparations from wild-type, R9AP $^{-/-}$, and R7BP(RhoCT)::R9AP $^{-/-}$ transgenic animals were measured as described in Materials and Methods. ***B***, The rate constants of transducin GTPase activity were determined by exponential fits of the data presented in ***A*** and plotted as bars. The resulting k_{app} values were 0.078 $\pm$ 0.007 s $^{-1}$ for wild-type, 0.040 $\pm$ 0.002 s $^{-1}$ for R9AP $^{-/-}$, and 0.050 $\pm$ 0.001 s $^{-1}$ for R7BP(RhoCT)::R9AP $^{-/-}$. ***C***, Effects of recombinant R7BP on RGS7•Gβ5-stimulated GTPase activity of lipid-modified Gα_o. Single-turnover GTPase activity of recombinant Gα_o was measured by single-turnover assays. Intrinsic GTPase activities of Gα_o in the presence of either empty Sf9 cell membranes or membranes expressing R7BP(R9APCT) were indistinguishable. However, when the reaction was supplemented with RGS7•Gβ5, GTPase activity was higher with the addition of the R7BP-containing membranes. Data were fitted with single exponents to derive the apparent rate constants (k_{app}). The k_{GAP} values were obtained by subtracting the rates of the intrinsic GTPase activity of Gαo observed in the absence of RGS proteins and plotted in ***D***. Error bars are means $\pm$ SEM.

outer segments and toward an alternative destination: the plasma membrane of the cell. This signal is not contained within the C-terminal sequence consisting of the Ras-like motif of a polybasic stretch followed by a palmitoylated cysteine doublet, which was previously demonstrated to be very efficient at targeting R7BP to plasma membranes (Drenan et al., 2005; Song et al., 2006), because replacement of this region by the transmembrane segment did not alter its plasma membrane localization and exclusion from the outer segment. We speculated that the targeting sequence is instead contained within the only other structural element of R7BP: the four-helical bundle that constitutes the RGS binding site. Interestingly, similar escape from the default pathway was described for the presynaptic protein syntaxin (Baker et al., 2008) that shares many common features with R7BP and R9AP, including the presence of the N-terminal four-helical bundle, suggesting that the presence of the specific sequences in this structural element could be responsible for dictating intracellular destinations of membrane anchors and similarly organized SNARE proteins.

In addition to passive targeting mechanisms, photoreceptor cells employ vesicular trafficking pathways for selective delivery of membrane proteins to the outer segments (Papermaster, 2002; Deretic, 2006). These pathways involve recognition of specific targeting signals that direct sorting of constituent proteins to vesicles bound to the outer segment. Two classes of such signals have been identified in photoreceptor proteins. The V(I)xPx motif is present in opsins and retinol dehydrogenase (Tam et al., 2000; Luo et al., 2004) and the second is found in peripherin/RDS (Tam et al., 2004). In this study, we show that V(I)xPx targeting signal contained within the C terminus of mouse rhodopsin is capable of rerouting R7BP to the outer segments. Notably, the C terminus of rhodopsin does not entirely switch localization of R7BP away from the plasma membrane but rather redistributes a significant portion of the protein to an alternative destination: the disc membranes of the outer segment. This observation suggests a nonexclusive mode of vesicular sorting in photoreceptors when two competing targeting signals can direct the same protein to multiple destinations in the polarized cells. It also suggests that separation of the protein localization between discs and plasma membrane compartments involves a sorting process that relies on the recognition of passive and active targeting signals in substrate proteins.

Interestingly, we find that most of the R7BP immunofluorescence in outer segments of R7BP(RhoCT) rods appear to be distributed in a gradient fashion with the higher concentration of the protein being present at the base of the structure. Similar observations were made with the proteins containing V(I)xPx motif and anchored to the membrane via palmitoylation (Tam et al., 2000; Luo et al., 2004). Since no gradient distribution is observed for transmembrane R9AP or rhodopsin and because protein palmitoylation is known to be a highly labile modification, we think that gradient distribution of R7BP could be explained by previously suggested inefficient palmitoylation in the outer segments (Luo et al., 2004). Proteins that loose palmitoyl moiety and have no other means of membrane attachment would become soluble and could be translocated back to the cell body and the inner segment by a passive diffusion mechanism described for transducin subunits (Calvert et al., 2006; Artemyev, 2008).

Finally, the data allows us, for the first time, to unequivocally conclude that RGS9-1•Gβ5 complex is not targeted independently, and that the action of membrane anchor R7BP or R9AP is both necessary and sufficient for determining its subcellular destination. A previous study showed that the deletion of the DEP domain in RGS9-1 that eliminates its binding to R9AP and R7BP also disrupts targeting of the truncated protein to the outer segments (Martemyanov et al., 2003). However, the possibility remained that the elements necessary for the targeting are contained within the DEP domain itself. Therefore, by showing that RGS9-1•Gβ5 complex can be competitively rerouted depending entirely on the identity of the membrane anchoring subunits, we establish the irreplaceable role of R7BP/R9AP in mediating RGS9-1 targeting in photo-

receptors. Together, these observations suggest that the identity of the membrane anchor reflects an adaptation of the GAP complex to effectively reach its unique intracellular destination in neurons to achieve efficient regulation of G-protein signaling.

References

Anderson GR, Posokhova E, Martemyanov KA (2009) The R7 RGS protein family: multi-subunit regulators of neuronal G protein signaling. Cell Biochem Biophys 54:33–46.

Artemyev NO (2008) Light-dependent compartmentalization of transducin in rod photoreceptors. Mol Neurobiol 37:44–51.

Baker SA, Martemyanov KA, Shavkunov AS, Arshavsky VY (2006) Kinetic mechanism of RGS9-1 potentiation by R9AP. Biochemistry 45:10690–10697.

Baker SA, Haeri M, Yoo P, Gospe SM 3rd, Skiba NP, Knox BE, Arshavsky VY (2008) The outer segment serves as a default destination for the trafficking of membrane proteins in photoreceptors. J Cell Biol 183:485–498.

Blundell J, Hoang CV, Potts B, Gold SJ, Powell CM (2008) Motor coordination deficits in mice lacking RGS9. Brain Res 1190:78–85.

Burns ME, Arshavsky VY (2005) Beyond counting photons: trials and trends in vertebrate visual transduction. Neuron 48:387–401.

Burns ME, Pugh EN Jr (2009) RGS9 concentration matters in rod phototransduction. Biophys J 97:1538–1547.

Calvert PD, Strissel KJ, Schiesser WE, Pugh EN Jr, Arshavsky VY (2006) Light-driven translocation of signaling proteins in vertebrate photoreceptors. Trends Cell Biol 16:560–568.

Cao Y, Song H, Okawa H, Sampath AP, Sokolov M, Martemyanov KA (2008) Targeting of RGS7/Gbeta5 to the dendritic tips of ON-bipolar cells is independent of its association with membrane anchor R7BP. J Neurosci 28:10443–10449.

Cao Y, Masuho I, Okawa H, Xie K, Asami J, Kammermeier PJ, Maddox DM, Furukawa T, Inoue T, Sampath AP, Martemyanov KA (2009) Retina-specific GTPase accelerator RGS11/Gbeta5S/R9AP is a constitutive heterotrimer selectively targeted to mGluR6 in ON-bipolar neurons. J Neurosci 29:9301–9313.

Chen CK, Burns ME, He W, Wensel TG, Baylor DA, Simon MI (2000) Slowed recovery of rod photoresponse in mice lacking the GTPase accelerating protein RGS9-1. Nature 403:557–560.

Cowan CW, Wensel TG, Arshavsky VY (2000) Enzymology of GTPase acceleration in phototransduction. Methods Enzymol 315:524–538.

Deretic D (2006) A role for rhodopsin in a signal transduction cascade that regulates membrane trafficking and photoreceptor polarity. Vision Res 46:4427–4433.

Deretic D, Williams AH, Ransom N, Morel V, Hargrave PA, Arendt A (2005) Rhodopsin C terminus, the site of mutations causing retinal disease, regulates trafficking by binding to ADP-ribosylation factor 4 (ARF4). Proc Natl Acad Sci U S A 102:3301–3306.

Drenan RM, Doupnik CA, Boyle MP, Muglia LJ, Huettner JE, Linder ME, Blumer KJ (2005) Palmitoylation regulates plasma membrane-nuclear shuttling of R7BP, a novel membrane anchor for the RGS7 family. J Cell Biol 169:623–633.

Drenan RM, Doupnik CA, Jayaraman M, Buchwalter AL, Kaltenbronn KM, Huettner JE, Linder ME, Blumer KJ (2006) R7BP augments the function of RGS7/Gbeta5 complexes by a plasma membrane-targeting mechanism. J Biol Chem 281:28222–28231.

Gold SJ, Hoang CV, Potts BW, Porras G, Pioli E, Kim KW, Nadjar A, Qin C, LaHoste GJ, Li Q, Bioulac BH, Waugh JL, Gurevich E, Neve RL, Bezard E (2007) RGS9-2 negatively modulates L-3,4-dihydroxyphenylalanine-induced dyskinesia in experimental Parkinson's disease. J Neurosci 27:14338–14348.

Grabowska D, Jayaraman M, Kaltenbronn KM, Sandiford SL, Wang Q, Jenkins S, Slepak VZ, Smith Y, Blumer KJ (2008) Postnatal induction and localization of R7BP, a membrane-anchoring protein for regulator of G protein signaling 7 family-Gbeta5 complexes in brain. Neuroscience 151:969–982.

Hooks SB, Waldo GL, Corbitt J, Bodor ET, Krumins AM, Harden TK (2003) RGS6, RGS7, RGS9, and RGS11 stimulate GTPase activity of Gi family G-proteins with differential selectivity and maximal activity. J Biol Chem 278:10087–10093.

Hu G, Wensel TG (2002) R9AP, a membrane anchor for the photoreceptor GTPase accelerating protein, RGS9-1. Proc Natl Acad Sci U S A 99:9755–9760.

Hu G, Zhang Z, Wensel TG (2003) Activation of RGS9-1GTPase acceleration by its membrane anchor, R9AP. J Biol Chem 278:14550–14554.

Jayaraman M, Zhou H, Jia L, Cain MD, Blumer KJ (2009) R9AP and R7BP: traffic cops for the RGS7 family in phototransduction and neuronal GPCR signaling. Trends Pharmacol Sci 30:17–24.

Karan S, Zhang H, Li S, Frederick JM, Baehr W (2008) A model for transport of membrane-associated phototransduction polypeptides in rod and cone photoreceptor inner segments. Vision Res 48:442–452.

Keresztes G, Mutai H, Hibino H, Hudspeth AJ, Heller S (2003) Expression patterns of the RGS9-1 anchoring protein R9AP in the chicken and mouse suggest multiple roles in the nervous system. Mol Cell Neurosci 24:687–695.

Keresztes G, Martemyanov KA, Krispel CM, Mutai H, Yoo PJ, Maison SF, Burns ME, Arshavsky VY, Heller S (2004) Absence of the RGS9/Gbeta5 GTPase-activating complex in photoreceptors of the R9AP knockout mouse. J Biol Chem 279:1581–1584.

Kizhatil K, Baker SA, Arshavsky VY, Bennett V (2009) Ankyrin-G promotes cyclic nucleotide-gated channel transport to rod photoreceptor sensory cilia. Science 323:1614–1617.

Kovoor A, Seyffarth P, Ebert J, Barghshoon S, Chen CK, Schwarz S, Axelrod JD, Cheyette BN, Simon MI, Lester HA, Schwarz J (2005) D2 dopamine receptors colocalize regulator of G-protein signaling 9-2 (RGS9-2) via the RGS9 DEP domain, and RGS9 knock-out mice develop dyskinesias associated with dopamine pathways. J Neurosci 25:2157–2165.

Krispel CM, Chen CK, Simon MI, Burns ME (2003) Prolonged photoresponses and defective adaptation in rods of Gbeta5 $^{-/-}$ mice. J Neurosci 23:6965–6971.

Krispel CM, Chen D, Melling N, Chen YJ, Martemyanov KA, Quillinan N, Arshavsky VY, Wensel TG, Chen CK, Burns ME (2006) RGS expression rate-limits recovery of rod photoresponses. Neuron 51:409–416.

Lem J, Applebury ML, Falk JD, Flannery JG, Simon MI (1991) Tissue-specific and developmental regulation of rod opsin chimeric genes in transgenic mice. Neuron 6:201–210.

Lishko PV, Martemyanov KA, Hopp JA, Arshavsky VY (2002) Specific binding of RGS9-Gbeta5L to protein anchor in photoreceptor membranes greatly enhances its catalytic activity. J Biol Chem 277:24376–24381.

Luo W, Marsh-Armstrong N, Rattner A, Nathans J (2004) An outer segment localization signal at the C terminus of the photoreceptor-specific retinol dehydrogenase. J Neurosci 24:2623–2632.

Makino ER, Handy JW, Li T, Arshavsky VY (1999) The GTPase activating factor for transducin in rod photoreceptors is the complex between RGS9 and type 5 G protein beta subunit. Proc Natl Acad Sci U S A 96:1947–1952.

Martemyanov KA, Arshavsky VY (2004) Kinetic approaches to study the function of RGS9 isoforms. Methods Enzymol 390:196–209.

Martemyanov KA, Arshavsky VY (2009) Chapter 7: biology and functions of the RGS9 isoforms. Prog Mol Biol Transl Sci 86:205–227.

Martemyanov KA, Lishko PV, Calero N, Keresztes G, Sokolov M, Strissel KJ, Leskov IB, Hopp JA, Kolesnikov AV, Chen CK, Lem J, Heller S, Burns ME, Arshavsky VY (2003) The DEP domain determines subcellular targeting of the GTPase activating protein RGS9 in vivo. J Neurosci 23:10175–10181.

Martemyanov KA, Yoo PJ, Skiba NP, Arshavsky VY (2005) R7BP, a novel neuronal protein interacting with RGS proteins of the R7 family. J Biol Chem 280:5133–5136.

Martemyanov KA, Krispel CM, Lishko PV, Burns ME, Arshavsky VY (2008) Functional comparison of RGS9 splice isoforms in a living cell. Proc Natl Acad Sci U S A 105:20988–20993.

Masuho I, Celver J, Kovoor A, Martemyanov KA (2010) Membrane anchor R9AP potentiates GTPase-accelerating protein activity of RGS11/Gbeta5 complex and accelerates inactivation of the mGluR6-Go signaling. J Biol Chem 285:4781–4787.

Nishiguchi KM, Sandberg MA, Kooijman AC, Martemyanov KA, Pott JW, Hagstrom SA, Arshavsky VY, Berson EL, Dryja TP (2004) Defects in RGS9 or its anchor protein R9AP in patients with slow photoreceptor deactivation. Nature 427:75–78.

Panicker LM, Zhang JH, Posokhova E, Gastinger MJ, Martemyanov KA, Simonds WF (2010) Nuclear localization of the G protein beta 5/R7-

regulator of G protein signaling protein complex is dependent on R7 binding protein. J Neurochem 113:1101–1112.

Papermaster DS (2002) The birth and death of photoreceptors: the Friedenwald lecture. Invest Ophthalmol Vis Sci 43:1300–1309.

Pepperberg DR, Cornwall MC, Kahlert M, Hofmann KP, Jin J, Jones GJ, Ripps H (1992) Light-dependent delay in the falling phase of the retinal rod photoresponse. Vis Neurosci 8:9–18.

Pugh EN Jr (2006) RGS expression level precisely regulates the duration of rod photoresponses. Neuron 51:391–393.

Rahman Z, Schwarz J, Gold SJ, Zachariou V, Wein MN, Choi KH, Kovoor A, Chen CK, DiLeone RJ, Schwarz SC, Selley DE, Sim-Selley LJ, Barrot M, Luedtke RR, Self D, Neve RL, Lester HA, Simon MI, Nestler EJ (2003) RGS9 modulates dopamine signaling in the basal ganglia. Neuron 38: 941–952.

Shi G, Yau KW, Chen J, Kefalov VJ (2007) Signaling properties of a short-wave cone visual pigment and its role in phototransduction. J Neurosci 27:10084–10093.

Skiba NP, Martemyanov KA, Elfenbein A, Hopp JA, Bohm A, Simonds WF, Arshavsky VY (2001) RGS9-Gbeta5 substrate selectivity in photoreceptors: opposing effects of constituent domains yield high affinity of RGS interaction with the G protein-effector complex. J Biol Chem 276: 37365–37372.

Sondek J, Siderovski DP (2001) Ggamma-like (GGL) domains: new frontiers in G-protein signaling and beta-propeller scaffolding. Biochem Pharmacol 61:1329–1337.

Song JH, Waataja JJ, Martemyanov KA (2006) Subcellular targeting of RGS9-2 is controlled by multiple molecular determinants on its membrane anchor, R7BP. J Biol Chem 281:15361–15369.

Song JH, Song H, Wensel TG, Sokolov M, Martemyanov KA (2007) Localization and differential interaction of R7 RGS proteins with their membrane anchors R7BP and R9AP in neurons of vertebrate retina. Mol Cell Neurosci 35:311–319.

Tam BM, Moritz OL, Hurd LB, Papermaster DS (2000) Identification of an outer segment targeting signal in the COOH terminus of rhodopsin using transgenic *Xenopus laevis*. J Cell Biol 151:1369–1380.

Tam BM, Moritz OL, Papermaster DS (2004) The C terminus of peripherin/rds participates in rod outer segment targeting and alignment of disk incisures. Mol Biol Cell 15:2027–2037.

Traynor JR, Terzi D, Caldarone BJ, Zachariou V (2009) RGS9-2: probing an intracellular modulator of behavior as a drug target. Trends Pharmacol Sci 30:105–111.

Tsang SH, Burns ME, Calvert PD, Gouras P, Baylor DA, Goff SP, Arshavsky VY (1998) Role for the target enzyme in deactivation of photoreceptor G protein in vivo. Science 282:117–121.

Zachariou V, Georgescu D, Sanchez N, Rahman Z, DiLeone R, Berton O, Neve RL, Sim-Selley LJ, Selley DE, Gold SJ, Nestler EJ (2003) Essential role for RGS9 in opiate action. Proc Natl Acad Sci U S A 100:13656–13661.